

## BACKSTEPPING ADAPTIVE NEURAL NETWORK CONTROL FOR UNMANNED SURFACE VESSEL COURSE TRACKING

YONGSHENG ZHAO\*, CUNHE LI, GUOFENG WANG AND YUNSHENG FAN

College of Information Science and Technology  
Dalian Maritime University  
No. 1, Linghai Road, Dalian 116026, P. R. China  
\*Corresponding author: yszhao@dlnu.edu.cn

Received July 2016; accepted October 2016

**ABSTRACT.** *Considering the modeling errors, environment disturbances and rudder characteristics, the course-controlling of unmanned surface vessel (USV) is a nonlinear control problem with unmatched and uncertainties. In order to solve the above problems, this paper presents an adaptive RBF neural network (ARBFNN) controller which is combined with the technology of backstepping and ARBFNN. In the process of controller design, only one neural network is used to approximate the whole unknown dynamics which contain modeling errors and environment disturbances. It is theoretically proved that the proposed ARBFNN controller can make the USV track the designed heading angle and turning rate with arbitrary accuracy, while guaranteeing the uniform ultimate boundedness of the closed-loop course tracking control system of USV. Comparative studies are carried out between the proposed control scheme and the traditional PD control under the same conditions, and the results show that the proposed control scheme has a better performance.*

**Keywords:** USV, ARBFNN, Backstepping, Rudder characteristics, Course control

1. **Introduction.** Unmanned surface vessel (USV), as an intelligent motion platform, can be widely used in hydrographic survey, channel detection, environment monitoring, modern warfare, etc. [1,2]. In actual marine environment, USVs are affected by sea wind, current, waves, and other interference factors [3]. The hull various hydrodynamic coefficients will change with the speed change which makes the USV has nonlinear, uncertainty and time-varying characteristics. Therefore, the course tracking of USV with the characteristics of the rudder is an unmatched uncertain nonlinear control problem. In this case, traditional PID control cannot meet the demands of the USV navigation control [4].

With the development of nonlinear control theory, backstepping approach is introduced to design course controller. An adaptive robust course control algorithm is proposed by incorporating the technique of integrator into backstepping design [5]. Combining Nussbaum gain technique with backstepping algorithm, a nonlinear adaptive controller is designed without prior knowledge about sign of uncertain control coefficient [6]. However, there always exist uncertainty problems in the actual maneuvers of ship, such as modeling errors and unknown external environment disturbance. So many adaptive backstepping algorithms based on neural networks and fuzzy systems are widely used in the design of the course controller [7,8]. Based on the dynamic surface control and neural networks, a direct adaptive neural networks controller is proposed for a class of uncertain nonlinear SISO systems in the presence of input saturation and applied to ship steering control [9]. However, the existence of hydraulic serving system for steering engine causes the problem of the lag of control input. So in order to get a better control effect, it is needed to consider the servo characteristics of actuator in the design of course controller. In addition, a single neural network and a single fuzzy approximation approach are presented for a class of uncertain strict-feedback nonlinear systems in [10,11], respectively. Following

this approach, the structure of the designed controller is simpler and the computational burden is lighter.

Based on the backstepping technique and adaptive RBF neural network (ARBFNN), this paper proposes a novel adaptive tracking control algorithm for USV course-controlling with characteristics of the rudder and system uncertainties. The RBF neural network is used as an approximation for the system uncertainties including modeling errors and external disturbances. The main advantages of the proposed controller are that: (1) the characteristics of the rudder are considered; (2) only one neural network is used to approximate the lumped unknown function of the course-controlling system at the last step of backstepping. Using Lyapunov stability theory, the uniformly ultimately boundedness of all signals in the closed-loop system is proven. The goal of course-changing adaptive tracking control of USV is realized. At last the correctness and robustness of the proposed control algorithm are verified through simulation.

This paper is organized as follows. Section 2 presents the mathematical model of USV. Section 3 develops, in specific, the design of an ARBFNN controller. Section 4 presents the simulation for the proposed method. Section 5 contains conclusions.

## 2. Problem Formulation and Preliminaries.

**2.1. Problem formulation.** Considering the influence of the modeling errors and environment disturbances, the uncertain nonlinear mathematical model of USV is expressed as

$$T\ddot{\psi} + \dot{\psi} + \alpha\psi^3 + \lambda_1(\psi, \dot{\psi}) = K\delta + w_1 \quad (1)$$

where  $\psi$  is heading angle,  $\delta$  is rudder angle,  $\alpha$  is called Norrbin coefficient,  $\lambda_1$  is modeling errors,  $w_1$  is equivalent disturbance rudder angle of the environment disturbances due to wind, waves and currents, and  $K$  and  $T$  are the gain constant and time constant, respectively.

The rudder servo characteristics can be regarded as a small closed loop servo system. Considering the modeling errors and external disturbances, the mathematical model can be described as

$$\dot{\delta} = -\delta/T_E + K_E\delta_E/T_E + \lambda_2(\delta, \delta_E) + w_2 \quad (2)$$

where  $K_E$  is control gain of rudder,  $T_E$  is time constant of rudder, and  $\delta_E$  is rudder order for steering control.

From April to September 2015, the USV of Dalian Maritime University's "LanXin" were a large number of direct sailing, turning, and zigzag manipulation tests [12,13]. With experimental data obtained on-site, the manipulation parameters of USV can be identified by using the least-squares method as follows:  $K = 0.707$ ,  $T = 0.332$ ,  $K_E = 1$ ,  $T_E = 0.2$  and  $\alpha = 0.001$ .

**Assumption 2.1.** *The USV's smooth reference trajectory  $\psi_r$  and its first 2 derivatives  $\dot{\psi}_r$ ,  $\ddot{\psi}_r$  are known and bounded.*

**Assumption 2.2.** *The modeling errors  $\lambda_1$  and  $\lambda_2$  are unknown and environment disturbances  $w_1$  and  $w_2$  are unknown and bounded.*

**2.2. RBF neural network.** RBF neural network can be divided into three layers: the input layer, the hidden layer and the output layer. It is a feed-forward network, which has a strong ability of online self-learning. It can approximate the nonlinear function with any accuracy, and has a fast convergence rate.

The Gauss function is chosen as the basis function of the neural network in this paper. The expression of Gauss function is

$$\phi_i(x) = \exp \left[ -\frac{(x - c_i)^T(x - c_i)}{2\sigma_i^2} \right], \quad i = 1, 2, \dots, q \quad (3)$$

where  $\phi_i$  is the output of the  $i$  hidden node,  $\sigma_i$  is the generalized constant of the hidden node,  $q$  is the number of the  $i$  hidden nodes,  $x = [x_1, x_2, \dots, x_M]^T$  is the input samples, and  $c_i$  is the center vector of Gauss function of the  $i$  hidden node,  $c_i = [c_{i1}, c_{i2}, \dots, c_{iM}]^T$ .

RBF neural network realizes the nonlinear mapping of the input layer to the output layer. The output of the network can be described as

$$y_k = \sum_{i=1}^q w_{ki} \phi_i (\|x - c_i\|^2), \quad i = 1, 2, 3, \dots, q \tag{4}$$

where  $y_k$  is the output of the  $k$  node of the output layer, and  $w_{ki}$  is the weight coefficient of the hidden layer to the output layer.

**Lemma 2.1.** *The universal approximation properties show that any real continuous function  $f(x)$  on a compact set  $\Omega_x \subset R^M$  can be approximated by an RBF neural network to arbitrary accuracy. This can be expressed as*

$$f(x) = W^{*T} \phi(x) + \varepsilon(x) \quad \forall x \in \Omega_x \subset R^M \tag{5}$$

where  $W^*$  is the ideal weight vector of RBF neural network, and  $\varepsilon(x)$  is the approximation error between the ideal approximation value and actual function value.

$$W^* := \arg \min_{W \in R^q} \left\{ \sup_{x \in \Omega_2} |f(x) - W^T \phi(x)| \right\} \tag{6}$$

**Assumption 2.3.** *The ideal weight vector  $W^*$  of RBF neural network and the approximation error  $\varepsilon(x)$  between ideal approximation value and actual function value are bounded and this can be expressed as*

$$\|W^*\| \leq W_m, \quad |\varepsilon(x)| \leq \varepsilon_m \quad \forall x \in \Omega_x \tag{7}$$

where  $W_m$  and  $\varepsilon_m$  are positive constants.

**3. ARBFNN Controller Design.** First of all, define  $x_1 = \psi$ ,  $x_2 = \dot{\psi}$ ,  $x_3 = \delta$ ,  $u = \delta_E$ ,  $X = [x_1 \ x_2 \ x_3]^T$ . The USV's nonlinear mathematical model (1) can be rewritten as

$$\dot{x}_1 = x_2, \quad \dot{x}_2 = f_1(x_1, x_2) + g_1 x_3 + w_1, \quad \dot{x}_3 = f_2(x_3) + g_2 u + w_2 \tag{8}$$

where  $f_1(x_1, x_2) = -(x_2 + \alpha x_2^3 + \lambda_1)/T$  and  $f_2(x_3) = -x_3/T_E + \lambda_2$  are unknown nonlinear functions including modeling errors,  $g_1 = K/T$  and  $g_2 = K_E/T_E$  are gain constants which have identified, and  $w_1$  and  $w_2$  are unknown bounded environment disturbances.

**Theorem 3.1.** *For the reference signal  $\psi_r$ , consider the system (8) satisfying Assumptions 2.1 and 2.2. Suppose that the lumped unknown function  $d$  can be approximated by the RBF neural network in the sense that the approximating error is bounded. If the control law and the adaptive law are chosen as (21), then the actual course  $\psi$  can track a desired time-variant reference trajectory  $\psi_r$  with arbitrary accuracy and all the signals in the closed-loop system remain bounded.*

The proof on Theorem 3.1 consists of three steps.

**Step 1:** Define the tracking errors as  $z_1$ ,  $z_2$  and  $z_3$ .

$$z_1 = x_1 - \psi_r, \quad z_2 = x_2 - a_2, \quad z_3 = x_3 - a_3 \tag{9}$$

where  $a_2$  and  $a_3$  are virtual control laws.

Differentiating  $z_1$ , we have

$$\dot{z}_1 = x_2 - \dot{\psi}_r = z_2 + a_2 - \dot{\psi}_r \tag{10}$$

Consider a Lyapunov function candidate as  $V_1 = z_1^2/2$  and its time derivative is

$$\dot{V}_1 = z_1 \dot{z}_1 = z_1 (z_2 + a_2 - \dot{\psi}_r) \tag{11}$$

Design the virtual control law for (11) as

$$a_2 = -c_1 z_1 \quad (12)$$

where  $c_1 > 0$  is design parameter.

Substituting (12) into (11), we have

$$\dot{V}_1 = -c_1 z_1^2 + z_1 z_2 - z_1 \dot{\psi}_r \quad (13)$$

**Step 2:** Differentiating  $z_2$ , we have

$$\dot{z}_2 = \dot{x}_2 - \dot{a}_2 = f_1 + g_1 z_3 + g_1 a_3 + w_1 - \dot{a}_2 \quad (14)$$

Consider a Lyapunov function candidate as  $V_2 = V_1 + z_1^2/2$  and its time derivative is

$$\dot{V}_2 = \dot{V}_1 + z_2 \dot{z}_2 = -c_1 z_1^2 + z_1 z_2 - z_1 \dot{\psi}_r + z_2 (f_1 + g_1 z_3 + g_1 a_3 + w_1 - \dot{a}_2) \quad (15)$$

Design the virtual control law for (14) as

$$a_3 = -(z_1 + c_2 z_2)/g_1 \quad (16)$$

where  $c_2 > 0$  is design parameter.

Substituting (16) and (13) into (15), we have

$$\dot{V}_2 = -c_1 z_1^2 - c_2 z_2^2 - z_1 \dot{\psi}_r + z_2 (f_1 + g_1 z_3 + w_1 - \dot{a}_2) \quad (17)$$

**Step 3:** Differentiating  $z_2$ , we have

$$\dot{z}_3 = \dot{x}_3 - \dot{a}_3 = f_2 + g_2 u + w_2 - \dot{a}_3 \quad (18)$$

Define  $d = \left[ -z_1 \dot{\psi}_r + z_2 (f_1 + w_1 - \dot{a}_2) + z_3 (f_2 + w_2 - \dot{a}_3) \right] / z_3$ . Based on Lemma 2.1, the RBF neural network (5) can be employed to approximate the unknown term  $d$ .

Define  $x = \left[ x_1 \ x_2 \ x_3 \ z_1 \ z_2 \ z_3 \ \psi_r \ \dot{\psi}_r \right]^T$  and  $d$  as the input vector and output variable of the RBF neural network, respectively. The unknown term  $d$  can be expressed as

$$d = W^{*T} \phi(x) + \varepsilon \quad (19)$$

where  $W^*$  is the ideal weight vector of RBF neural network and  $\varepsilon$  denotes the minimum approximation error.

Consider the Lyapunov function candidate as  $V_3 = V_2 + z_3^2/2 + \tilde{W}^T \tilde{W} / (2\gamma)$  and its time derivative is

$$\begin{aligned} \dot{V}_3 &= -c_1 z_1^2 - c_2 z_2^2 - z_1 \dot{\psi}_r + z_2 (f_1 + g_1 z_3 + w_1 - \dot{a}_2) + z_3 (f_2 + g_2 u + w_2 - \dot{a}_3) \\ &\quad - \tilde{W}^T \dot{\tilde{W}} / \gamma \\ &= -c_1 z_1^2 - c_2 z_2^2 + z_3 (g_1 z_2 + d + g_2 u) - \tilde{W}^T \dot{\tilde{W}} / \gamma \end{aligned} \quad (20)$$

where  $\tilde{W} = W^* - \hat{W}$ ,  $\hat{W}$  is the estimate of the ideal weight vector  $W^*$  and  $\gamma$  is the positive design constant.

Design the actual control law and adaptive law for (20) as

$$u = - \left[ g_1 z_2 + c_3 z_3 + \hat{W}^T \phi(X) \right] / g_2, \quad \dot{\hat{W}} = \gamma \left[ z_3 \phi(X) + \kappa \hat{W} \right] \quad (21)$$

where  $c_3 > 0$  is a design parameter.

Substituting (21) and (17) into (20), we have

$$\begin{aligned} \dot{V}_3 &= -c_1 z_1^2 - c_2 z_2^2 - c_3 z_3^2 + z_3 \left[ \tilde{W}^T \phi(X) + \varepsilon \right] - z_3 \tilde{W}^T \phi(X) - \kappa \tilde{W}^T \hat{W} \\ &= -c_1 z_1^2 - c_2 z_2^2 - c_3 z_3^2 + z_3 \varepsilon - \kappa \tilde{W}^T \hat{W} \end{aligned} \quad (22)$$

According to the perfect square inequality and (7), we have

$$\varepsilon z_3 \leq (\varepsilon_m^2 + z_3^2) / 2 \quad (23)$$

$$-\kappa \tilde{W}^T \hat{W} \leq -\kappa \tilde{W}^T \tilde{W} / 2 + \kappa \|W^*\|^2 / 2 \leq -\kappa \tilde{W}^T \tilde{W} / 2 + \kappa W_m^2 / 2 \quad (24)$$

where  $\varepsilon_m$  and  $W_m$  represent the least upper bounds of  $|\varepsilon|$  and  $\|W^*\|$ , respectively.

Substituting (23) and (24) into (22), we have

$$\dot{V}_3 \leq -c_1 z_1^2 - c_2 z_2^2 - c_3 z_3^2 - \kappa \tilde{W}^T \tilde{W} / 2 + \varepsilon_m^2 / 2 + z_3^2 / 2 + \kappa W_m^2 / 2 \leq -aV_3 + C \quad (25)$$

where  $a = \min\{2c_1, 2c_2, 2c_3, \kappa\gamma\}$ ,  $C = \varepsilon_m^2 / 2 + z_3^2 / 2 + \kappa W_m^2 / 2$ .

Integrating the inequality (25) yields

$$0 \leq V_3(t) \leq C/a + [V_3(0) - C/a]e^{-at} \quad (26)$$

The above inequality (26) shows that  $V_3(t)$  is uniformly ultimately bounded. Then according to  $V_3 = V_2 + z_3^2 / 2 + \tilde{W}^T \tilde{W} / (2\gamma)$ ,  $z_1, z_2, z_3, \tilde{W}$  are uniformly ultimately bounded. Further, based on  $z_1 = \psi - \psi_r, z_2 = \dot{\psi} - a_2, z_3 = \delta - a_3$ , (12) and (16), we know that  $\psi, \dot{\psi}, a_2, a_3$  are bounded. Moreover, since  $\tilde{W}$  are bounded due to Assumption 2.3,  $\hat{W} = W^* - \tilde{W}$  are bounded. Thus, all signals in the closed loop course-controlling system are uniformly ultimately bounded.

Substituting  $V_3(t)$  into (26), we have

$$|z_1| \leq \sqrt{2C/a + 2[V(0) - C/a]e^{-at}} \quad (27)$$

For any given  $\varsigma_1 > \sqrt{2C/a}$ , there exists a constant  $T_1 > 0$  such that  $|z_1| \leq \varsigma_1$  for all  $t > T_1$ . Thus, the vessel heading angle error can converge to the compact set  $\Omega_1 = \{z \in R \mid |z| \leq \varsigma_1\}$ . Since  $\sqrt{2C/a}$  can be made arbitrarily small by suitably selecting design parameters  $c_1, c_2, c_3, \kappa, \gamma$ , the vessel can be maintained at the desired values of its heading angle with arbitrary accuracy.

Theorem 3.1 has been proved.

**4. The Simulation and Comparison Studies.** In this section, the simulations are carried out to validate the proposed ARBFNN controller for USV's course tracking. In addition, performance comparisons between the proposed ARBFNN controller and traditional PD controller under the same parameters are conducted to assess the adaptability and robustness of the proposed control scheme. The proposed ARBFNN controller (21) for course tracking is tested on "LanXin" USV in two cases.

**4.1. ARBFNN controller.** The design parameters of ARBFNN controller are chosen as:  $c_1 = 4, c_2 = 15, c_3 = 20, \kappa = 0.01, \gamma = 1$ . The modeling errors and environment disturbances are set as  $\lambda_1 = 0.04\dot{e} + 0.1e, w_1 = 0.1 \sin t \cos(0.2t), \lambda_2 = 0.2\delta + 0.1\delta_E, w_2 = 0.2H$ , and  $H$  is Gauss white noise after two order filters. The input vector of the RBF neural network is  $x = [x_1 \ x_2 \ x_3 \ z_1 \ z_2 \ z_3 \ \psi_r \ \dot{\psi}_r]^T$ . The design parameters of network are chosen as: node number  $q = 20$ , the centers  $c_i$  ( $i = 1, 2, \dots, 20$ ) evenly spaced in  $[-3.2 \ 3.2] \times [-1.6 \ 1.6] \times [-0.62 \ 0.62] \times [-1 \ 1] \times [-1 \ 1] \times [-1 \ 1] \times [-1 \ 1] \times [-1 \ 1]$  and the width  $\sigma_i = 5$  ( $i = 1, 2, \dots, 20$ ). The following simulations are carried out.

**Case 1:** The simulation results without modeling errors and environment disturbances are depicted using solid line in Figures 1(a) to 1(f). The reference heading angles used in simulation study are chosen as  $\psi_r = 90^\circ$  and  $\psi_r = 30 \sin(0.2t)$ , respectively.

**Case 2:** The simulation results in the presence of modeling errors and environment disturbances are depicted using solid line in Figures 2(a) to 2(f). The reference heading angles used in simulation study are  $\psi = 90^\circ$  and  $\psi = 30 \sin(0.2t)$ , respectively.

From Figures 1(a) and 1(b), it is observed that the ARBFNN controller can force the actual heading angle  $\psi$  and turning rate  $r$  of the USV to arrive the reference heading angle  $\psi_r$  and zero in around 5s, respectively. Figure 1(d) shows that the actual heading angle  $\psi$  asymptotically tracks the reference heading angle  $\psi_r$  with high accuracy and Figure 1(e) presents the change of turning rate  $r$ . The control rudder angle  $\delta$  is shown in Figures 1(c) and 1(f) which illustrate the change of rudder angle  $\delta$  in  $\psi_r = 90^\circ$  and  $\psi_r = 30 \sin(0.2t)$ . Figure 2 shows that the actual heading angles are still able to track the reference heading angle in the presence of modeling errors and environment disturbances. The above results

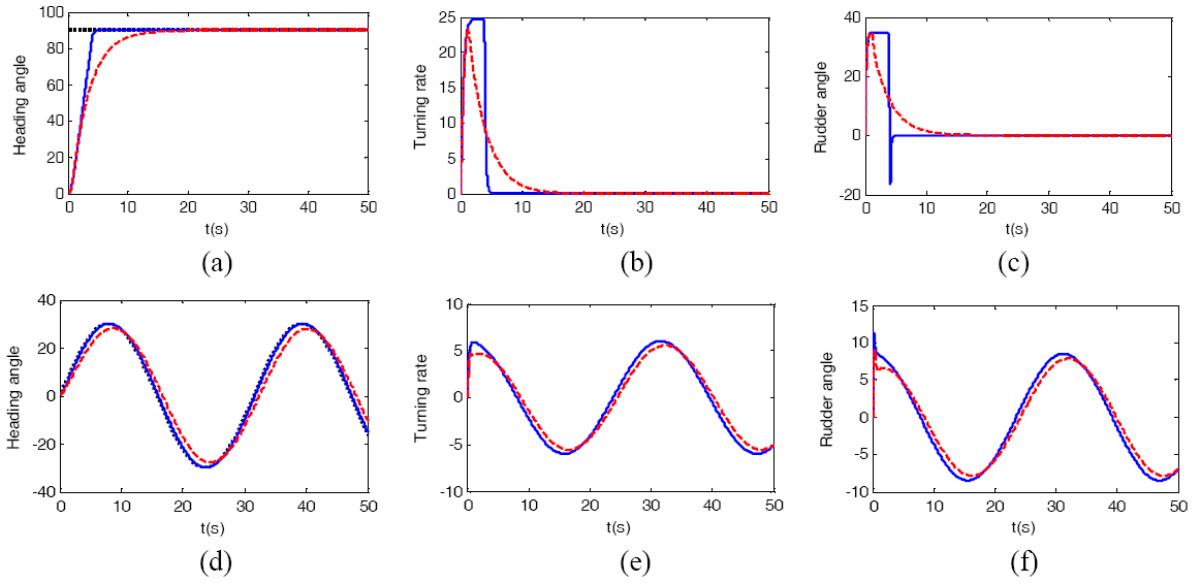


FIGURE 1. Case 1 (the comparison simulation results between ARBFNN controller and PD controller)  $\psi_r = 90^\circ$ : (a) heading angle; (b) turning rate; (c) rudder angle;  $\psi_r = 30 \sin(0.2t)$ : (d) heading angle; (e) turning rate; (f) rudder angle

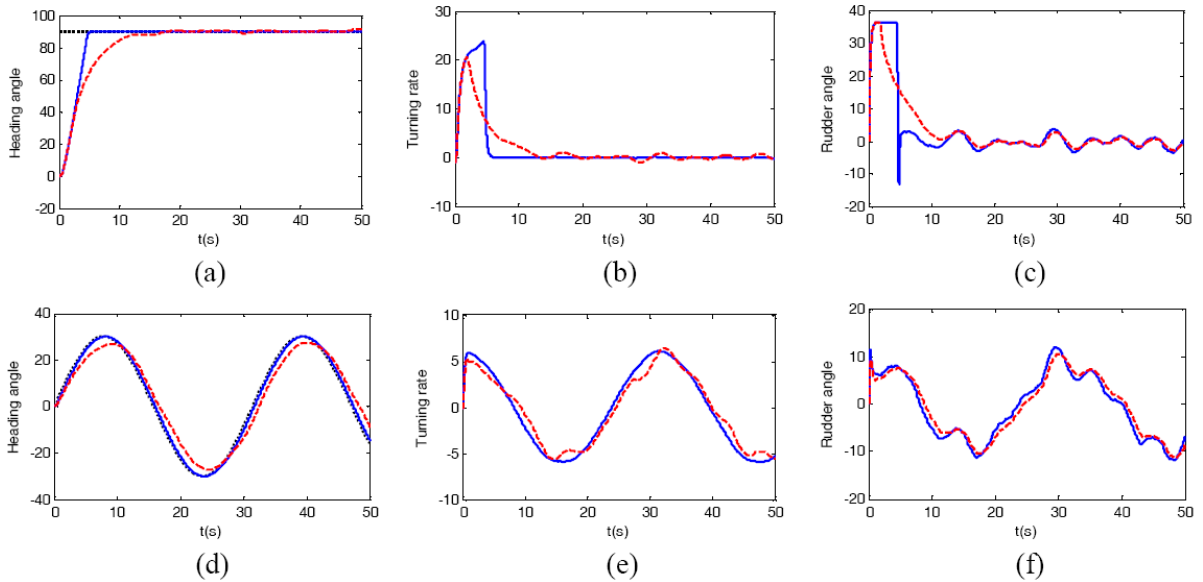


FIGURE 2. Case 2 (the comparison simulation results in the presence of modeling errors and environment disturbances)  $\psi_r = 90^\circ$ : (a) heading angle; (b) turning rate; (c) rudder angle;  $\psi_r = 30 \sin(0.2t)$ : (d) heading angle; (e) turning rate; (f) rudder angle

reveal that the ARBFNN controller can implement USV's course-controlling and has the robustness against uncertain environment disturbances and adaptability to uncertain modeling errors.

**4.2. Traditional PD controller.** In this subsection, we will compare the performance of the proposed control scheme with that traditional PD control (28).

$$\delta_{PD} = k_p e(t) + k_d \dot{e}(t) \quad (28)$$

where  $\delta_{PD}$  is controlled quantity output of PD controller, and  $k_p = 1.2$  and  $k_d = 2.4$  are the proportionality coefficient and differential coefficient, respectively.  $e(t)$  is heading

angle error. The simulation studies for the PD controller are carried out in two cases in Section 4.1. The simulation results are depicted using dashed line in Figure 1 and Figure 2.

In order to further compare the effects of ARBFNN controller and PD controller, the performance indexes are set as: the regulation time  $T_e$ , the evaluation function of course tracking errors  $\Theta_e = \int_0^\infty |\psi - \psi_r| dt$ , the evaluation function of actual steering angle  $J_e = \int_0^\infty |\delta| dt$ . The greater the  $\Theta_e$  is, the worse the performance of the course control is; the greater the  $J_e$  is, the greater the energy consumption is. The performance indexes of the ARBFNN controller and PD controller are summarized in Table 1.

TABLE 1. Performance indexes of ARBFNN controller and PD controller

Performance index		ARBFNN controller		PD controller	
		Case 1	Case 2	Case 1	Case 2
$\psi_r = 90^\circ$	$T_e/s$	5	5	15	15
	$\Theta_e$	210	255	318	388
	$J_e$	134	226	127	215
$\psi_r = 30 \sin(0.2t)$	$\Theta_e$	58	59	187	204
	$J_e$	278	304	254	292

The data of Table 1 display that the traditional PD controller can keep the USV at the desired target value in around; however, the steady-state performance of the PD controller under modeling errors and environment disturbances becomes unsatisfactory. In case 2, the PD controller cannot eliminate tracking errors. In two cases, the energy consumption of ARBFNN controller is slightly greater than the PD controller.

**5. Conclusions.** In this paper, an ARBFNN controller is developed for the course-controlling system of USV with the characteristics of rudder in the presence of modeling errors and environment disturbances. The proposed controller guarantees the uniformly ultimately boundness of the closed-loop system. Adaptive updating laws of the proposed controller are designed to against unknown bound environment disturbances and adapt to uncertain modeling errors. The proposed scheme performance has been confirmed by simulation results. Simulation results and simulation comparisons prove that the proposed course-controlling controller has superior adaptability for modeling errors and good robustness against disturbances. In future work, input saturation constraints will be considered to handle the possible instability problem based on the existing course control system of USV.

**Acknowledgment.** This work is supported by the Natural Science Foundation of Liaoning Province of China under Grant 2015020022, Fundamental Research Funds for the Central Universities under Grant 3132014321, 3132016312. The authors would like to thank the reviewers for their helpful comments and suggestions, which have helped us to improve the presentation.

**REFERENCES**

[1] R. Zhang, P. P. Tang, Y. M. Su et al., An adaptive obstacle avoidance algorithm for unmanned surface vehicle in complicated marine environments, *IEEE/CAA Journal of Automatica Sinica*, vol.1, no.4, pp.385-396, 2014.

[2] S. Cambell, W. Naeem and G. W. Irwin, A review on improving the autonomy of unmanned surface vehicles through intelligent collision avoidance manoeuvres, *Annual Reviews in Control*, vol.36, no.2, pp.267-283, 2012.

[3] B. Volker, *Unmanned Surface Vehicles – A Survey*, Skibsteknisk Selskab, Copenhagen, Denmark, 2008.

- [4] T. I. Fossen, *Recent Developments in Ship Control Systems Design*, Sterling Publications Limited, London, 2000.
- [5] Y. Y. Lin, J. L. Du and J. Niu, Design of backstepping based adaptive robust nonlinear controller of ship course, *Ship Engineering*, vol.29, no.1, pp.24-27, 2007.
- [6] J. L. Du, J. Zhao, Y. B. Wu et al., Adaptive robust nonlinear control design for course-tracking of ships based on dynamic surface control, *Proc. of the 32nd Chinese Control Conference*, pp.519-524, 2013.
- [7] Y. Liu and C. Guo, RBF neural network based adaptive nonlinear control for ship course keeping, *Journal of Dalian Maritime University*, vol.39, no.4, pp.1-4, 2013.
- [8] D. J. Zhu, N. Ma and X. C. Gu, Adaptive fuzzy compensation control for nonlinear ship course-keeping, *Journal of Shanghai Jiao Tong University*, vol.49, no.2, pp.250-254, 2015.
- [9] J. F. Li and T. S. Li, Direct adaptive neural network tracking control with input saturation, *Journal of Applied Sciences*, vol.31, no.3, pp.294-302, 2013.
- [10] G. Sun, D. Wang, T. S. Li et al., Single neural network approximation based adaptive control for a class of nonlinear systems in strict-feedback form, *Nonlinear Dynamics*, vol.72, no.1, pp.175-184, 2013.
- [11] Z. M. Xiao, T. S. Li and Z. F. Li, A novel single fuzzy approximation based adaptive control for a class of uncertain strict-feedback discrete-time nonlinear systems, *Neurocomputing*, vol.167, pp.179-186, 2015.
- [12] Y. S. Fan, X. J. Sun, G. F. Wang and C. Guo, On fuzzy self-adaptive PID control for USV course, *Proc. of the 34th Chinese Control Conference*, Hangzhou, China, pp.8472-8478, 2015.
- [13] Y. S. Fan, Z. L. Ge, Y. S. Zhao and G. F. Wang, Design of information network and control system for USV, *SICE Annual Conference*, Hangzhou, China, pp.1391-1396, 2015.